Agricultural and Forest Meteorology 272–273 (2019) 118–127

Contents lists available at ScienceDirect

Agricultural and Forest Meteorology

journal homepage: www.elsevier.com/locate/agrformet

# Does direct-seeded rice decrease ecosystem-scale methane emissions?—A case study from a rice paddy in southeast China

Hong Li[a,b,c,1], Hai-Qiang Guo[a,1], Manuel Helbig[d], Sheng-Qi Dai[a], Meng-Shan Zhang[a], Min Zhao[e], Chang-Hui Peng[b,f,**], Xiang-Ming Xiao[g], Bin Zhao[a,*]

[a] Ministry of Education Key Laboratory for Biodiversity Science and Ecological Engineering, and Coastal Ecosystems Research Station of the Yangtze River Estuary, Fudan University, Shanghai 200433, China
[b] Department of Biology Science, Institute of Environment Sciences, University of Quebec at Montreal, Montreal C3H 3P8, Canada
[c] Key Laboratory of New Technology for Construction of Cities in Mountain Area, Faculty of Architecture and Urban Planning, Chongqing University, Chongqing 400045, China
[d] School of Geography and Earth Sciences, McMaster University, Hamilton L8S 4K1, Canada
[e] Shanghai Academy of Environmental Sciences, Shanghai 200233, China
[f] A&F University, Yangling, Shaanxi 712100, China
[g] Department of Botany and Microbiology, Center for Spatial Analysis, University of Oklahoma, Norman, Ok, USA

ARTICLE INFO

*Keywords:*
$CH_4$ flux
Seedling-transplanting
Direct-seeding
Eddy covariance
Gross ecosystem productivity

ABSTRACT

Rice paddy fields are one of the world's largest anthropogenic sources of methane ($CH_4$). With the largest area of rice paddy fields, China is experiencing a rapid shift from conventional seedling-transplanted rice (TPR) to direct-seeded rice (DSR) due to efforts to introduce labor-saving practices. However, the potential effect of this change on agricultural ecosystem $CH_4$ flux ($F_{CH4}$) are less studied and remain poorly understood. Here, we analyze $F_{CH4}$ measured with the eddy covariance technique over a rice paddy where TPR was applied in 2013 and DSR in 2016. Meteorological conditions (*i.e.*, friction velocity, radiation and temperature) between the two growing seasons were similar. However, compared to the TPR system, cumulative $CH_4$ emissions in the DSR system were 25% higher ($610.5 \pm 73.3$ vs $488.8 \pm 56.2$ kg $CH_4$ ha$^{-1}$). The increase in $CH_4$ emissions mainly occurred during the flooding periods (*i.e.* DOY 173–203 and 222–260). After eliminating the effect of differences in weather conditions and water management practices between the TPR and DSR systems, daily $CH_4$ emissions in the DSR system remained significantly higher than in the TPR system. Gross ecosystem productivity (GEP) and rice density were higher in the DSR system than in the TPR system. Cross correlation and wavelet coherence analyses showed that $F_{CH4}$ were significantly correlated to GEP. Thus, increased $CH_4$ emissions in the DSR system are most likely due to greater GEP, which was associated with higher rice plant density. With the rapid development of DSR, a scientifically sound reduced seeding density could be a promising strategy to reduce $CH_4$ emissions.

## 1. Introduction

Methane ($CH_4$) is the third most important greenhouse gas after water vapour and carbon dioxide. 11% of the total annual anthropogenic $CH_4$ emissions are emitted by rice paddies (Smith et al., 2007), which provide the dominant staple food crop for over 5 billion people worldwide. According to the Food and Agriculture Organization of the United Nations, 30% of the world's rice was produced in China from 1994 to 2014. Thus, much effort was put into decreasing the $CH_4$ emissions in this region. For example, novel agricultural management practices were introduced to mitigate $CH_4$ emissions, *e.g.* change of irrigation regime greatly decreased $CH_4$ emissions in China (Li et al., 2002). In recent years, water-saving rice crop establishment techniques were introduced, which could potentially reduce $CH_4$ emissions in irrigated rice paddies (Kumar and Ladha, 2011; Liu et al., 2015, 2014a; Malyan et al., 2016; Pathak et al., 2011).

* Corresponding author at: Ministry of Education Key Laboratory for Biodiversity Science and Ecological Engineering, and Coastal Ecosystems Research Station of the Yangtze River Estuary, Fudan University, Shanghai 200433, China
** Corresponding author.
*E-mail addresses:* peng.changhui@uqam.ca (C.-H. Peng), zhaobin@fudan.edu.cn (B. Zhao).
[1] Hong Li and Hai-Qiang Guo are equally contributing first authors.

https://doi.org/10.1016/j.agrformet.2019.04.005
Received 22 June 2018; Received in revised form 4 April 2019; Accepted 7 April 2019

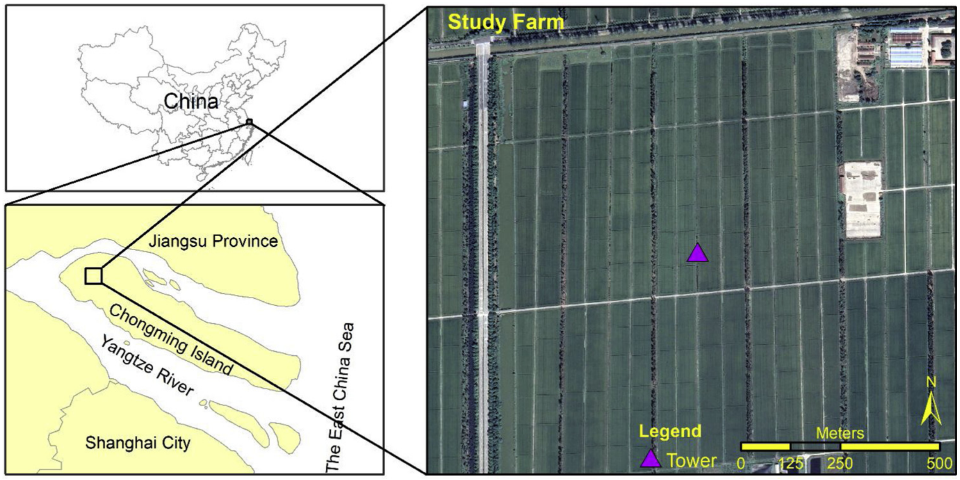


**Fig. 1.** Location and the satellite image (from Google Earth) taken on 1st October 2018 of the study area.

Direct-seeded rice (DSR) has been introduced to reduce water, save labour, and lower the risk of large $CH_4$ emissions. Worldwide, DSR rice cropping systems account for nearly 23% of the total rice cultivation area (Rao et al., 2007). In China, a rapid shift from traditional seedling-transplanted rice (TPR) to DSR occurred since the 1990s, with DSR mainly being used in the middle and lower reaches of the Yangtze River (Nie and Peng, 2017). In DSR, crops are established from seeds sown in the fields rather than by transplanting seedlings from the nursery. DSR includes dry seeding, which is sowing dry seeds into dry soil, wet seeding, which is sowing pregerminated seeds on puddled soil, and water seeding, where seeds are sown into standing water. To avoid potential yield decline problems, wet seeded rice with prolonged periods of flooding is widely grown in south China (Liu et al., 2014b), such as the water regime of moisture-flooding-midseason drainage-flooding-moisture irrigation (M-F-D-F-M) with alternating drying and wetting during the flooding periods. In China, wet seeding accounts for over 80% of the DSR planting area (Su et al 2014). The percentage of rice paddy area with wet DSR technology in Shanghai has risen from 65% in 1999 to 83% in 2008 (Chen and Chen, 2011) and continued increasing during the past decade (Gu et al., 2015; Liu, 2016; Wang et al., 2017).

The shift from TPR to DSR cropping systems could alter $CH_4$ emissions. Especially in dry DSR systems, under less anaerobic conditions, $CH_4$ emissions could be substantially reduced as compared to TPR, due to lower $CH_4$ production and release (Gupta et al., 2016; Hang et al., 2014; Kumar and Ladha, 2011). Kumar and Ladha (2011) integrated studies comparing $CH_4$ emissions from different crop establishment methods but with similar water management in rice, and concluded that $CH_4$ emissions were lower with wet- or dry-DSR than with TPR. Compared to TPR with continuous flooding, the reduction in $CH_4$ emissions ranged from 24% to 79% in dry-DSR and from 8% to 22% in wet-DSR (Kumar and Ladha, 2011). In China, Liu et al. (2014a) found that the wet DSR rice cropping system with a water regime of moist irrigation decreased $CH_4$ emissions by 39%, compared to a TPR system with a water regime of flooding-midseason drainage-flooding-moisture irrigation (F-D-F-M). However, most studies comparing the two establishment methods focused on dry DSR or wet DSR with a water regime of moist irrigation (Liu et al., 2015, 2014a), but not on the popular wet DSR with prolonged periods of flooding, which is more common in southern China.

Often, field measurements of $CH_4$ emissions rely on the use of the chamber technique. However, static chamber measurements are discrete in time and space, and may not capture the dynamics of $CH_4$ fluxes ($F_{CH4}$) on varying time scales, due to the high temporal and spatial variability of $F_{CH4}$ in rice paddies (Alberto et al., 2014; Kim et al., 2016; Knox et al., 2016; Meijide et al., 2011). In addition, chambers impact the turbulent mixing in the sampling area, which may lead to biases in $CH_4$ emission estimates (Dore et al., 2003; Krauss et al., 2016; Morin et al., 2017; Yu et al., 2013). In contrast, the eddy covariance (EC) technique provides continuous measurements integrating all ecosystem processes and over a larger part of the landscape, without disturbing gas exchange processes between biological sources and the atmosphere (Baldocchi et al., 2001). However, there are only few studies using the EC technique to measure $CH_4$ emissions from rice paddy fields (Alberto et al., 2015, 2014; Bhattacharyya et al., 2014; Detto et al., 2011; Ge et al., 2018; Hatala et al., 2012b; Kim et al., 2016; Knox et al., 2016, 2015; Meijide et al., 2017, 2011), with a lack of study sites and studies of crop establishment method effects on $F_{CH4}$ in China so far (Ge et al., 2018).

In this study, the eddy covariance technique was used to measure $F_{CH4}$ over the course of complete rice growing seasons for the TPR and DSR crop establishment methods in the same area in southeast China. The studied DSR was the popular wet seeded rice with prolonged periods of flooding. The main objectives of this study were to: 1) measure and quantify the $F_{CH4}$ over the course of rice growing season under both TPR and DSR; and 2) test the hypothesis that direct-seeded rice decreases methane emissions of a rice paddy.

## 2. Data and Methods

### 2.1. Site description

The study site is located at the Yuejin Farm on the Chongming Island, Shanghai, China (31° 48′ 37.54″N, 121° 15′ 0.43″E) (Fig. 1). As Chongming Island was an alluvial island, the topography of the entire island is nearly flat. The farm covers an area of 18.95 $km^2$. The region experiences a subtropical monsoon climate. The annual precipitation and mean air temperature were 1156.1 ± 190.6 mm and 17.1 ± 0.6 °C (1991–2012), respectively. The soil texture is silt loam. The organic carbon and total nitrogen in the topsoil (0–8 cm) are 20 g $kg^{-1}$ and 1.6 g $kg^{-1}$, respectively (Cui et al., 2012). The farmland was intensively cultivated. An annual paddy rice-winter wheat cropping rotation was practiced.

### 2.2. Cropping regime and water management

The cropping regime and water management at the rice paddy are representative of common practices in southeast China. After the wheat crop, the experimental fields are waterlogged with a shallow water depth of 0.5–2 cm during the fallow season. Chopped wheat straw at about 10 cm length is mixed into the soil layer when farmers plow in rice cropping systems.

For the seedling-transplanted rice (TPR) cropping system, seeds

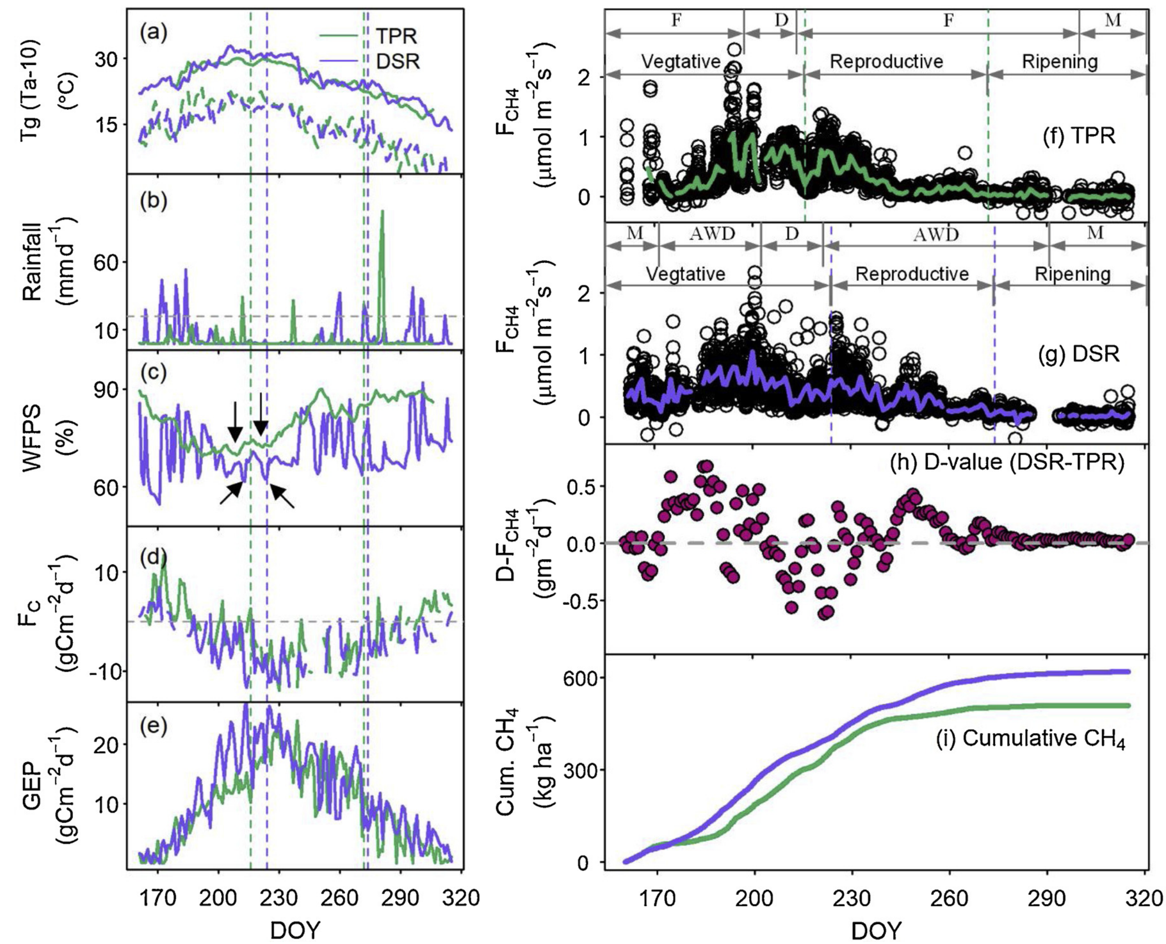


**Fig. 2.** Daily air temperature (a), rainfall (b), water filled pore space (WFPS) (c), $CO_2$ flux (d) and gross ecosystem production (GEP) (e), half hourly (f, g, black dots) and daily (f, g, lines) $F_{CH4}$ in DSR (*i.e.* 2016) (g) and TPR (*i.e.* 2013) (f) and their daily differences (h, red dots), and their cumulative $CH_4$ emissions (i) from DOY 161 to DOY 316. The TPR and DSR system are distinguished by the colours of green and purple, respectively (a, b, c, d, e, f, g, i). D-values (h) and cumulative $CH_4$ emissions (i) are derived from gap-filled fluxes. The positive difference-values (h) indicate that $CH_4$ emissions in the DSR are larger than in the TPR system. The gray dotted lines in (b) represent daily rainfall = 20 mm. The horizontal gray dotted lines in (c) and (h) are zero reference lines. The vertical green and purple dotted lines (a, b, c, d, e, f) indicate the growing stages of rice in the TPR and DSR system, respectively. The black arrows (c) show the mid-season drainage (For interpretation of the references to colour in this figure legend, the reader is referred to the web version of this article).

(*Oryza sativa* L., cv. Wuyunjing 31) were sown in a nursery bed on May 20 (DOY 140), and then seedlings were transplanted to the paddy fields on June 10 (DOY 161) and harvested on November 6 (DOY 310), 2013. In the TPR fields, transplanting ridge spacing was 0.20 × 0.15 m, with three seedlings per ridge. All the TPR fields were characterized by a typical water regime of continuous flooding-midseason drainage-re-flooding-moisture (F-D-F-M) irrigation during the rice-growing season (Fig. 2c). Initially, the level of flooding was kept from one week before rice transplantation until July 14 (DOY195), and was then manually drained for two short periods in the mid-season (from DOY202 to DOY214) (Fig. 2c). From then on, all the fields were re-flooded until October 26 (DOY 299), 2013, which was followed by maintaining soil moisture status but without waterlogging. 5–10 cm of standing water was kept in the fields during the flooding periods.

In the direct-seeded rice (DSR) cropping system, seeds of the rice cultivar Wuyunjing 31 were broadcast at the rate of 400 seeds m$^{-2}$ (representing the standard seed density for local DSR production, which was higher than in TPR system) on the wet soil surface on June 11 (DOY163), and harvested on November 11 (DOY 316), 2016. From 11th to 19th June, the field was kept moist but without waterlogging. The water was impounded starting June 20 (DOY 172). Several studies showed, alternate wetting and drying (AWD) can successfully maximize DSR grain yield and improve water productivity, compared to daily continuous irrigation (Chauhan et al., 2017; Sudhir-Yadav et al., 2011). To our knowledge, the AWD regime in wet DSR rice systems is very common in southeast China. In this farm, AWD irrigation (irrigated every 6–10 days once the field was not waterlogged anymore) was also employed to save water in the DSR system instead of being kept flooded. Thus, the water regime was moisture-AWD-midseason drainage-AWD-moisture irrigation (M-AWD-D-AWD-M). The mid-season drainage was applied from late July to early August (from DOY204 to 222).

Urea was broadcasted on the fields in both the TPR and DSR systems. The nitrogen fertilizer was used at a rate of 225 kg N ha$^{-1}$ and 250 kg N ha$^{-1}$ in the TPR and DSR system, respectively (for more details see Table 1). Calcium superphosphate, used as phosphate fertilizer

**Table 1**
N fertilizer application for the TPR and DSR paddy fields in 2013 and 2016, respectively.

| | TPR | DSR |
|---|---|---|
| Total nitrogen | 225 kg N ha$^{-1}$ | 250 kg N ha$^{-1}$ |
| 1$^{st}$ Base fertilizer | 20 % (9 June) | 19 % (10 June) |
| 2$^{nd}$ Base fertilizer | 22% (19 June) | 21% (20 June) |
| 3$^{th}$ fertilizer | 24% (23 June) | 24% (9 July) |
| 4$^{th}$ fertilizer | 19% (29 July) | 22% (24 July) |
| 5$^{th}$ fertilizer | 15% (8 August) | 18% (2 August) |

at a rate of 160 kg N $ha^{-1}$, was also applied as basal fertilizer in both the TPR and DSR systems. Herbicides were applied before transplanting in 2013, and on 29 June, 29 August and 12 September in 2016.

### 2.3. Flux and ancillary data

The eddy covariance (EC) technique was used to quantify net fluxes of $CO_2$ ($F_{CO2}$), GEP and $F_{CH4}$ between the rice paddy and atmosphere from 2013 to 2016. The flux tower was located in the center of Yuejin Farm (31° 48′ 37.54″N, 121° 15′ 0.43″E). The area was flat and uniform within 500 m radius from the tower during the rice growing season (Fig. 1). Sensors were mounted 3.3 m above the soil surface. The EC system included an open path $CO_2$/$H_2O$ infrared gas analyzer (LI-7500 A, LI − COR, Cor., Lincoln, NE, USA (LI − COR)), an open path $CH_4$ gas analyzer (LI-7700, LI − COR), and a sonic anemometer (CSAT3, Campbell Sci., Inc., Logan, UT, USA (CSI)). The turbulence data were sampled with a frequency of 10 Hz and collected by a data logger (CR5000, Campbell Scientific, Inc., USA).

$F_{CO2}$ and $F_{CH4}$ were calculated using the EddyPro 6.2.0 software (LI − COR). A despiking procedure including detecting and eliminating individual out-of-range values was applied (Vickers and Mahrt, 1997). The block average method was used to extract high-frequent fluctuation in the raw data. The time lag detection method used was covariance maximization with default. The double coordinate rotation method was applied to ensure the mean vertical wind speed was zero, averaged over 30 min (Wilczak et al., 2001). Compensation of Webb-Pearman-Leuning density fluctuations (WPL terms) was implemented following Webb et al. (1980). We applied spike detection of raw data after Vickers and Mahrt (1997). Spectral correction was performed after Moncrieff et al. (1997) (high-frequency).

The subsequent QA/QC processing was performed according to Li et al. (2018). The relative signal strength indicator (RSSI) was adopted to filter for periods when the mirror of LI-7700 was contaminated by rainfall or dust (RSSI < 20%). Data were removed when rainfall events occurred. In addition, we used friction velocity ($u$*) as a criterion for atmospheric mixing to ensure well-developed mixing conditions (Reichstein et al., 2005), and applied a threshold of $u^* > 0.12$ m $s^{-1}$. According to Foken et al. (2004), the steady state test and the well-developed turbulence test were used as quality flags. The test (1–9 system) provided the flag "1 - 3″ for high quality fluxes, "4 - 6″ for intermediate quality fluxes, and "9″ for poor quality fluxes (Foken et al., 2004). Thus, only data for which the quality flag < 7 were used for further analysis. The occasionally occurring sensor failures and quality criteria led to gaps of different duration. For the entire observation period, the data coverage after QA/QC was 72% for $F_{CO2}$ and 67% for $F_{CH4}$.

Gaps of $F_{CO2}$ and $F_{CH4}$ were filled using the marginal distribution sampling method (Helbig et al., 2017; Hommeltenberg et al., 2014; Reichstein et al., 2005). $F_{CO2}$ were further partitioned into gross ecosystem production (GEP) and ecosystem respiration (ER) with two methods. Nighttime used Reichstein et al., 2005 and daytime used Lasslop et al., 2010. GEP is presented with positive signs ($F_{CO2}$ = ER − GEP). The 'REddyProc_1.1.5′ R package was used.

Daily $F_{CH4}$ was obtained by averaging the quality-controlled half-hourly $F_{CH4}$ for each day. Because of quality control, rejection rates varied greatly from day to day. For reliable daily averages, only the days with gaps of less than 6 h were used.

The uncertainties of seasonal $F_{CH4}$ were obtained following Aurela et al. (2002). The random uncertainty for each half-hourly $CH_4$ flux was estimated through the empirical models described by Finkelstein and Sims, (2001). The uncertainty of gap-filling for $F_{CH4}$ was also estimated (Reichstein et al., 2005).

Micrometeorological and hydrological variables were measured concurrently, including rainfall (2 m above ground, TB4MM, Campbell Scientific Inc., Logan, UT, USA), air temperature (3.3 m above ground, HMP155 A, Campbell Scientific Inc., Logan, UT, USA), soil temperature (109, Campbell Scientific Inc., Logan, UT, USA) and volumetric water content at 5 cm depth (CS616, Campbell Scientific Inc., Logan, UT, USA). The volumetric water content was used to calculate soil water filled pore space (WFPS) using the formula: 100 × Volumetric Water Content ÷ (1 - soil bulk density ÷ soil particle density), soil particle density is assumed as 2.65 g $cm^{-3}$, soil bulk density was 1.01 g $cm^{-3}$.

### 2.4. Statistical analyses

A paired $t$-test was used to test for statistically significant differences ($\alpha$ = 0.05) in environmental conditions between the TPR and DSR system. Cross correlation analysis was used to find at which time lag two variables (*e.g.* $F_{CH4}$ & GEP) match (Bracewell et al., 1986; Papoulis and Maradudin, 1963). The cross-correlation of the two variables is maximum at a lag equal to the delay. A cross-correlation function ('ccf' in the 'acf' R package), which is a time series analysis tool, was used to compute the cross-correlation of two univariate time series (*e.g.* $F_{CH4}$ & GEP). The time lag k value (a, c) returned by ccf ($F_{CH4}$,GEP) estimates the correlation between $F_{CH4}$ [t + k] and GEP [t]. When one or more GEP [t] are predictors of $F_{CH4}$ [t + k], with k positive in x-axis (a, c), it indicates that GEP leads $F_{CH4}$.

Wavelet coherence (WTC) analysis allows investigating the cause and effect relationships between two time series variables at different time scales, a feature that a simple linear regression method cannot accomplish (Grinsted et al., 2004; Torrence and Compo, 1998). The coherence is a quantity between 0 and 1, which measures the cross correlation between two variables as a function of time frequency (Torrence and Compo, 1998). The WTC allows us to examine if the highest coherency areas in the frequency domain have a consistent phase angle, which indicates a phase-locked relationship between two variables. Such a phase-locked relationship in turn represents a causality, the dependence of one variable on another (Grinsted et al., 2004; Hatala et al., 2012a; Koebsch et al., 2015). For time periods with significant wavelet coherence, we used the phase angle to calculate the time lag (time lag = phase angle × wavelength ÷ 2$\pi$) between the correlated oscillations of the two series. The relative phase relationship is shown as arrows in the figures.

## 3. Results

### 3.1. Biological and environmental conditions during the study period

Daily air temperature ($p$ = 0.073), precipitation ($p$ = 0.061), net radiation ($p$ = 0.058) and friction velocity ($p$ = 0.49) between the rice growing seasons of 2013 and 2016 were not significantly different (Table 2). The wind rose in each growth stage between the TPR and DSR system were also similar (Fig. S1). In 2016 (*i.e.*, DSR), despite 344.7 mm higher seasonal amount of rainfall, daily soil water filled pore space (WFPS) was significantly smaller ($p$ < 0.001) than in 2013 (*i.e.*, TPR). The DSR system had *ca.* 11% less soil water content than the TPR system (Table 2). For the entire growing season, daily 10 cm soil temperature was significantly lower in the TPR than the DSR system (Table 2). Only on DOY 188–189, DOY 201–241 and DOY 296–301, the differences in soil temperature were larger than 1 °C between the two systems. However, no significant ($p$ = 0.15) difference was found between the TPR and the DSR system when DOY 201–241 were excluded (Fig. 2a, Table 2). Seasonal total aboveground biomass increased due to the higher rice plant density in the DSR, despite the rice yield being lower than in the TPR system (Table 2). Compared to the TPR cropping system, daily GEP increased significantly ($p$ < 0.001) in the DSR system.

### 3.2. Seasonal variation and $F_{CH4}$ magnitude

The seasonal pattern of $F_{CH4}$ in the DSR cropping system was similar to the pattern in the TPR cropping system, except for the first 10 days

**Table 2**
Air temperature (Ta), soil temperature at 10 cm depth (Tg), net radiation (Rn), rainfall, soil water filled pore space (WFPS), gross ecosystem productivity (GEP), rice seed density (Density), aboveground total biomass(Biomass), rice yield(Yield), and methane flux ($F_{CH4}$) from seedling-transplanted (DOY 161–310 in 2013, TPR) and direct-seeded (DOY 163–316 in 2016, DSR) rice cropping seasons. A paired *t*-test is used to test for statistically significant differences (Stat, $\alpha$ = 0.05) in these environmental and flux variables between the TPR and DSR system from DOY 161 to DOY 316. 'Y' and 'N' represent significant and not-significant, respectively. 'NF_$F_{CH4}$' and '$F_{CH4}$' represent $CH_4$ flux before and after gap-filling, respectively.

| | No. days | Ta range | Ta mean | Tg mean | Rn mean | Rainfall sum | WFPS mean | GEP mean | Density mean | Biomass sum | Yield sum | NF_$F_{CH4}$ mean | $F_{CH4}$ mean | $F_{CH4}$ sum | $F_{CH4}$/Yield sum |
|---|---|---|---|---|---|---|---|---|---|---|---|---|---|---|---|
| | (d) | (°C) | (°C) | (°C) | (W $m^{-2}$) | (mm) | (%) | (kg C $ha^{-1}$) | seeds $m^{-2}$ | (Mg $ha^{-1}$) | (Mg $ha^{-1}$) | (kg $CH_4$ $ha^{-1}$) | | | (kg $Mg^{-1}$) |
| TPR | 150 | 13.8˜33.2 | 25.1 | 25.2 | 139.3 | 353.5 | 80 | 99.4 | 100 | ˜10.5 | 7.2 | 3.3 | 3.3 | 488.8 | 67.9 |
| DSR | 154 | 13.6˜32.1 | 25.0 | 25.6 | 131.7 | 698.2 | 71 | 110.8 | 400 | ˜18.2 | 5.5 | 3.9 | 4.0 | 610.5 | 111.0 |
| Stat | | | N | Y[#] | N | N | Y | Y | | | | Y | Y | | |

[#] Not significant when DOY 201–241 were excluded.

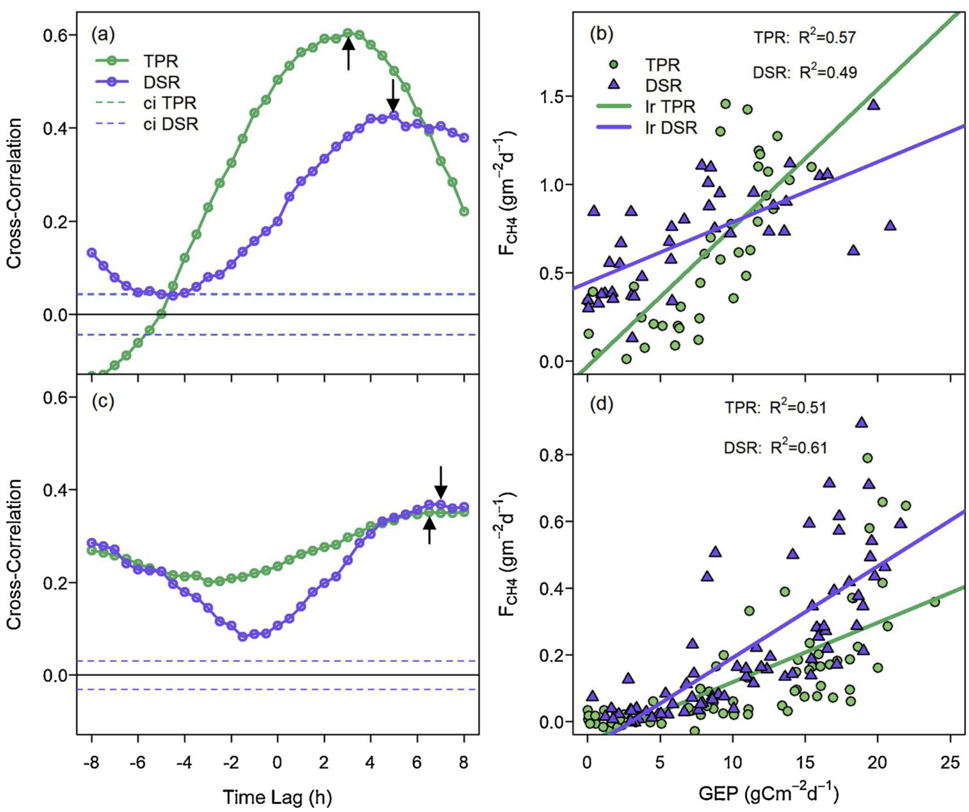


**Fig. 3.** The cross-correlation (a, c) of half hourly methane fluxes ($F_{CH4}$) and GEP, and the regression (b, d) of daily average $F_{CH4}$ and GEP indicate a close relationship between $F_{CH4}$ and GEP in the TPR (green) and DSR (purple) system before (a, b) and after (c, d) the mid-season drainage. The time lag k value (a, c) returned by ccf ($F_{CH4}$,GEP) estimates the correlation between $F_{CH4}$ [t + k] and GEP [t]. When one or more GEP [t] are predictors of $F_{CH4}$ [t + k], with k positive in x-axis (a, c), it indicates that GEP leads $F_{CH4}$. In this study, the maximum values of cross correlation before (a) and after (c) the midseason drainage occur when GEP leads $F_{CH4}$ 3 and 6.5 h in the TPR system (green oval), and 5 and 7 h in the DSR system (purple oval), respectively. The dotted lines (a, c) represent the confidence interval (confidence interval = 0.95) limits. (For interpretation of the references to colour in this figure legend, the reader is referred to the web version of this article).

(Fig. 2f, g). Daily $F_{CH4}$ started to increase when the field was flooded for the first time (10th and 20th June 2013 and 2016 respectively) until the peak fluxes were achieved, about 30˜40 days after rice transplantation in the TPR and after sowing in the DSR. $F_{CH4}$ reached a maximum of 1.5 g $CH_4$ $m^{-2}$ $d^{-1}$ on 13nd July in the TPR and 1.5 g $CH_4$ $m^{-2}$ $d^{-1}$ on 18th July in the DSR. In the middle season, $F_{CH4}$ exhibited a sharp decrease in both the TPR and DSR system. A secondary peak was observed in both cropping systems during the re-flooding period in August. Then, from late September until the end of the growing season, $F_{CH4}$ remained low (95% of the daily average fluxes were less than 0.1 ± 0.02 g $m^{-2}$ $d^{-1}$) (Fig. 2f, g). The main difference in the seasonal pattern between the DSR and TPR system was that $F_{CH4}$ in the DSR were small only during the nursery stage (˜first 10 days, *i.e.* DOY 163–172; except for 3 days with heavy rainfall) while the TPR system started to increase $CH_4$ emissions once the rice was transplanted.

Seasonal $CH_4$ emissions in the DSR cropping system were larger than in the TPR cropping system (Table 2 and Fig. 2). Growing season $F_{CH4}$ averaged 0.32 μmol $m^{-2}$ $s^{-1}$ and 0.26 μmol $m^{-2}$ $s^{-1}$ in the DSR and TPR system, respectively. The paired *t*-test showed that daily-averaged $F_{CH4}$ increased significantly ($p <$ 0.01) in the DSR compared to the TPR system. After gap-filling, the significant ($p <$ 0.001) increase remained in daily-averaged $F_{CH4}$. Seasonal cumulative $CH_4$ emissions were estimated at 610.5 ± 73.3 kg $CH_4$ $ha^{-1}$ and 488.8 ± 56.2 kg $CH_4$ $ha^{-1}$ in the DSR and TPR cropping system, respectively (Table 2 and Fig. 2i). Thus, the DSR system increased the seasonal $CH_4$ emissions by about 25% (24.9%) compared to the TPR. The increase in $CH_4$ emissions mainly occurred during the flooding (or AWD in the DSR) periods, *i.e.* DOY 173–203 and 222–260 (Fig. 2h). The duration of the growing season in the DSR system (154 days) was longer than in the TPR system (150 days). Even if the $CH_4$ emissions during the nursery stage (11th to 19th in June) of the DSR system were excluded, the seasonal $CH_4$ emissions of the DSR cropping system (145 days) were still about 25% (24.6%) larger than in the TPR system (150 days).

### 3.3. Controls on $F_{CH4}$ in DSR and TPR

Variations in $F_{CH4}$ depended on the artificial water management practices and rainfall. No significant positive linear correlation between $F_{CH4}$ and water filled pore space (WFPS) was found during the rice growing season, even when time lags were considered for both half-hourly and daily averaged data. Meanwhile, $F_{CH4}$ was relatively low (about 0.25 g $CH_4\ m^{-2}\ d^{-1}$) during the nursery stage in the DSR system when the soil was kept moist but not waterlogged (Fig. 2g). Also, a strong decrease in $F_{CH4}$ was observed with decreasing WFPS after draining occurred in the middle season (Fig. 2c, f, g). $F_{CH4}$ increased mostly 1–2 days after heavy rainfall events (daily rainfall > 20 mm) (Fig. 2b, f, g). For example, there was a heavy rainfall event on 12 June 2016 with a cumulative precipitation of 24.6 mm. $F_{CH4}$ quickly increased and reached 0.85 $g\ m^{-2}\ d^{-1}$ on 13 June. Meanwhile, fertilization and weed control practices did not result in significant variation. No significant correlation was found between $F_{CH4}$ and friction velocity ($u^*$) in both systems as the turbulence in this site was well developed.

The cross correlation analysis showed that half hourly $F_{CH4}$ was significantly correlated to half hourly GEP before the mid-season drainage in the TPR (Fig. 3a, DOY 161–202, $p < 0.05$, r = 0.60, When GEP led $F_{CH4}$ 3 h) and DSR system (Fig. 3a, DOY 163–204, $p < 0.05$, r = 0.43, When GEP led $F_{CH4}$ 5 h). Although the cross-correlation coefficient after the mid-season drainage was relatively lower than before the drainage, the correlation between $F_{CH4}$ and GEP was significant in both the TPR (Fig. 3c, DOY 220–310, $p < 0.05$, r = 0.35, When GEP led $F_{CH4}$ 6.5 h) and DSR system (Fig. 3c, DOY 225–316, $p < 0.05$, r = 0.37, When GEP led $F_{CH4}$ 7 h). In addition, daily average regression (Fig. 3b, d) also showed that daily average $F_{CH4}$ significantly increased with GEP before the mid-season drainage (Fig. 3b, $R^2$ = 0.57 and 0.49 in the TPR and DSR system, respectively) and after the mid-season drainage (Fig. 3d, $R^2$ = 0.51 and 0.61 in the TPR and DSR system, respectively).

### *3.4. $F_{CH4}$ after excluding the effect of different weather conditions and water management practices*

To eliminate the effect of different weather conditions and water management practices between the TPR and DSR systems, data were grouped into two parts, *i.e.* the periods with different rainfall, soil temperature and water management (DRTW) (Fig. 4a) and non-DRTW periods (Fig. 4b, c). DRTW periods in this study include days during midseason drainage, the first 10 days of the DSR system (DOY 163–172), days when D-value of soil temperature > 1℃ (DOY 188–189, DOY 201–241 and DOY 296–301), and heavy rainfall days (daily rainfall > 20 mm) together with the following one day (this threshold was determined by the lagged effect of rainfall on WFPS, Fig. S2) just after heavy rainfall.

Compared to the TPR system, $F_{CH4}$ in the DSR decreased 11.9% during the nursery stage in fields and midseason drainage practice periods (Fig. 4a). $F_{CH4}$ during the heavy rainfall periods accounted for 5% and 8.5% of the seasonal total amount of $F_{CH4}$ in 2013 and 2016, respectively. During the periods with different rainfall, the increase of $CH_4$ emissions in the DSR system comparing to the TPR system was 16.3 kg $CH_4\ ha^{-1}$, which was only 3% (much less than 25%) of the cumulative $CH_4$ emissions (488.8 kg $CH_4\ ha^{-1}$) in the TPR system. Although the difference (> 1 ℃) in daily soil temperature between the TPR and DSR system occurred on DOY 188–189, DOY 201–241 and DOY 296–301, the increase of soil temperature in the DSR system did not result in the increase of $CH_4$ emissions compared to the TPR system (Fig. 2a, h).

Meanwhile, non-DRTW daily $F_{CH4}$ remained significantly ($p < 0.001$) larger in the DSR compared to the TPR system (Fig. 4b). Non- DRTW daily $F_{CH4}$ exhibited a strong exponential dependence on 10 cm soil temperature (Tg) (Fig. 4b, $R^2$ = 0.85 and 0.75 in the TPR and DSR system, respectively) in the rice paddy. The DSR emitted more methane than the TPR system for the same soil temperature. The regression models in the TPR and DSR are $F_{CH4} = 4.2e\text{-}05e^{0.33\times Tg}$, and $F_{CH4} = 2.7e\text{-}04e^{0.29\times Tg}$, respectively. Considering the differences in the rice plant density and biomass between the TPR and DSR systems, $F_{CH4}$ in the DSR system was normalized (*i.e.*, $F_{CH4} \div 18.2 \times 10.5$ in the DSR. 18.2 and 10.5 were the biomass sum in the DSR and TPR system, respectively) (Fig. 4c). After the normalization, no significant ($p$ = 0.47) increase in daily $F_{CH4}$ was observed between the DSR and TPR system. The regression model in the DSR was $F_{CH4} = 1.6e\text{-}04e^{0.29\times Tg}$. The $Q_{10}$ which didn't change before and after the normalization were 27.1 and 18.2 in the TPR and DSR system, respectively.

In sum, compared to the TPR system, the decrease of $CH_4$ emissions in the DSR system during the first 10 days and from DOY 207–225 (Figs. 2h and 4 a) was exceeded by the increase during the flooding (or AWD in the DSR) periods, resulting in seasonal cumulative $CH_4$ emissions in the DSR system that were 25% higher. Moreover, this increase was not caused by the differences in rainfall, soil temperature and water management.

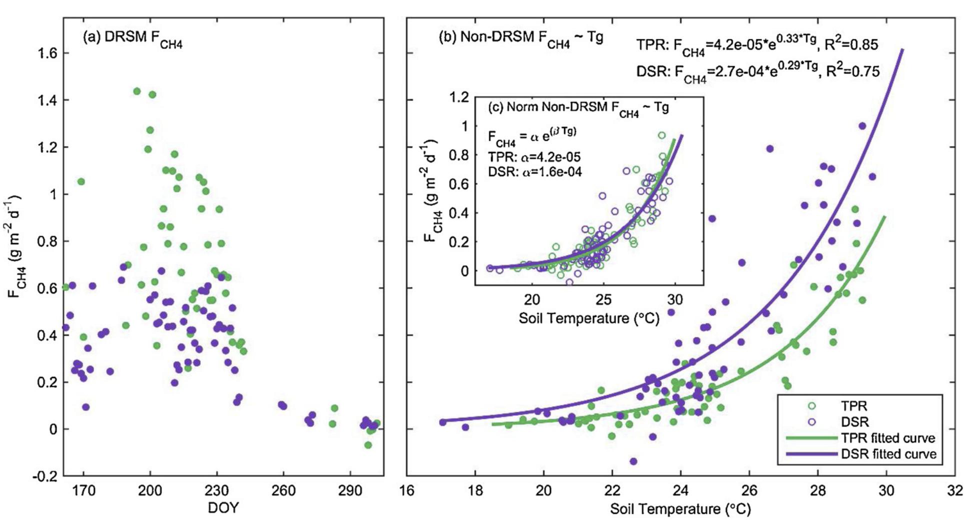


**Fig. 4.** Daily average methane fluxes ($F_{CH4}$) between the TPR (2013, green) and DSR (2016, purple) systems during the periods with (a) and without (b, c) different rainfall, soil temperature and water management (DRTW). DRTW periods in this study include days during midseason drainage, the first 10 days of the DSR system (DOY 163–172), days when D-value of soil temperature > 1℃ (DOY 188–189, DOY 201–241 and DOY 296–301), and heavy rainfall days (daily rainfall > 20 mm) together with the following one day (the period was decided by the lagged effect of rainfall on WFPS, Fig. S2) just after heavy rainfall. The data during the periods without DRTW shows exponential dependence on daily 10 cm soil temperature ($T_g$) of daily $F_{CH4}$ (b). The separate model parameters are fitted for the TPR (green lines) and DSR (purple lines) systems. Regression models for the daily averaged $F_{CH4}$ and $T_g$ in TPR and DSR are: $F_{CH4} = 4.2e\text{-}05e^{0.33\times Tg}$ (1), $Q_{10}$ = 27.1, n = 70, $R^2$ = 0.85, $p < 0.001$; and $F_{CH4} = 2.7e\text{-}04e^{0.29\times Tg}$ (2), $Q_{10}$ = 18.2, n = 67, $R^2$ = 0.75, $p < 0.001$, respectively. Considering the differences in the rice plant density and biomass between the TPR and DSR systems, $F_{CH4}$ in the DSR is normalized (*i.e.*, $F_{CH4} \div 18.2 \times 10.5$ in the DSR) (c). The regression models are also $F_{CH4} = \alpha \times e^{\beta\times Tg}$. The 'α' are estimated at 4.2e-05 and 1.6e-04 for the TPR and the DSR system, respectively. The 'β' are same as before the normalization (*i.e.*, 0.33 in the TPR, 0.29 in the DSR) (c). (For interpretation of the references to colour in this figure legend, the reader is referred to the web version of this article).

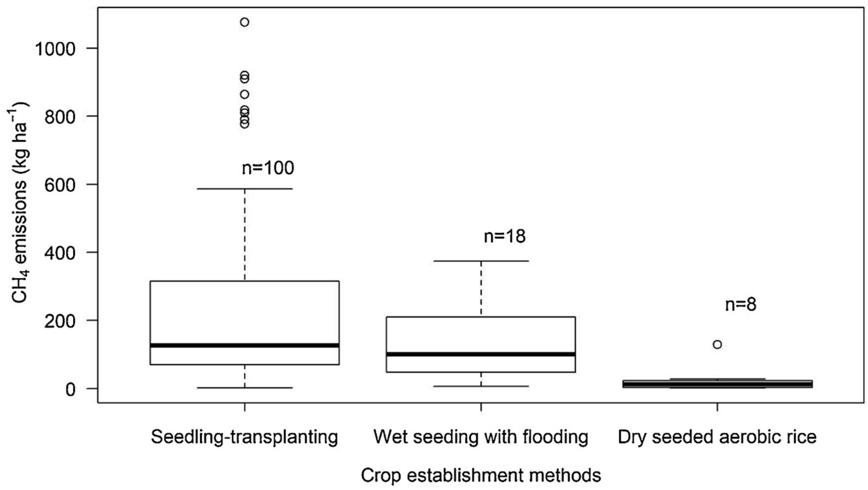


**Fig. 5.** Effects of various crop establishment methods on methane emissions (Data compiled from reports shown in Text S1).

## 4. Discussion

### 4.1. Seasonal variation and magnitude of $F_{CH4}$ in the rice paddy

With both DSR and TPR, the rice paddy acted as a strong $CH_4$ source (488.8 and 610.5 kg $CH_4$ ha$^{-1}$) during the rice growing season. These seasonal $CH_4$ emissions were within the range but at the higher end of most reported $CH_4$ emissions from rice paddies (Ge et al., 2018; Fig. 5). However, the seasonal patterns of $CH_4$ emissions in the TPR rice cropping systems were generally comparable to those previously reported on conventional rice paddies under a similar water regime of FDFM in southeast China (Hou et al., 2012; Liu et al., 2014a; Zou et al., 2005). Similarly, the seasonal patterns of the DSR cropping system were similar to those reported for water regimes of M-F-D-F-M (Hang et al., 2014; Zhang et al., 2012). For example, in a rice paddy in Jiangsu Province, China (Zhang et al., 2012), $CH_4$ emissions were also reported to peak before the mid-season drainage with a secondary peak after the mid-season drainage.

However, in our case study, the hypothesis that direct-seeded rice decreases methane emissions of a rice paddy was not supported. In contrast to most previous studies (Gupta et al., 2016; Kumar and Ladha, 2011; Liu et al., 2014a), our results showed that $CH_4$ emissions in the DSR system were significantly larger than in the TPR system.

### 4.2. Effects of rice establishment methods on $CH_4$ emissions

Lower soil water content in the DSR system should decrease $CH_4$ emissions instead of contributing to the increase of $CH_4$ emissions compared to the TPR system. Anaerobic soil conditions, which depend on water content in rice fields, are a prerequisite for $CH_4$ production by methanogens in rice paddies. This dependence on anaerobic conditions could explain why $F_{CH4}$ decreased during the middle season drainage and increased after a heavy precipitation in both rice systems. Moreover, compared to the TPR system, lower WFPS during the first 10 days and from DOY 207–225 led to lower $CH_4$ emissions in the DSR system (Figs. 2h and 4 a). Other studies reported that compared to TPR cropping systems, seasonal $CH_4$ emissions decreased in dry DSR and the wet DSR with moist irrigation cropping systems, mainly due to less anaerobic conditions in these DSR systems (Gupta et al., 2016; Liu et al., 2014a; Pathak, 2012). Similar to these studies, Tao et al. (2016) found that wet DSR with prolonged periods of flooding also largely decreased $CH_4$ emissions when they controlled an ideal condition that the seedling density was same in the TPR and DSR system. However, in our study site, the rice plants density was different between the TPR and DSR system. Except for the periods of nursery stage and middle season drainage, daily $F_{CH4}$ significantly increased in the DSR compared to the TPR system, while $F_{CH4}$ was not driven by WFPS.

The hypothesis that direct-seeded rice decrease methane emissions of a rice paddy is not supported here. To demonstrate that this does not contradict previous findings, we synthesized $CH_4$ emissions from previous studies comparing $CH_4$ emissions of TPR and DSR cropping systems. Although dry DSR strongly decreased $CH_4$ emissions, no significant difference existed between TPR and wet DSR with prolonged periods of flooding systems (Fig. 5). Dry DSR cropping systems often keep aerobic conditions with no standing water throughout the season, resulting in aerobic conditions limiting anaerobic $CH_4$ production in the rice paddy (Kumar and Ladha, 2011; Sandhu and Kumar, 2016). Dry DSR production is practiced traditionally in rainfed upland ecosystems in Asian countries, but is rare in irrigated areas (Kumar and Ladha, 2011). In contrast to dry seeded aerobic rice, wet DSR with prolonged periods of flooding, which is typical for many irrigated areas, often creates more anaerobic conditions favoring enhanced $CH_4$ production (Fig. 6).

The increase of $CH_4$ emissions in the DSR cropping system compared to the TPR system appears not to be caused by differences in environmental conditions, water and fertilizer management practices and their differences between 2013 and 2016. Soil temperature is an important factor regulating the seasonality of $F_{CH4}$ (Conrad, 2007, 1996; Helbig et al., 2017; Yvon-Durocher et al., 2014). For the studied rice paddy, we also found an exponential dependence of $F_{CH4}$ on air / soil temperature (Fig. 4b). However, mean air / soil temperature between the growing seasons of 2013 and 2016 were very similar (Table 2). Although the difference (> 1 °C) in daily soil temperature between the TPR and DSR system occurred on some days, the increase of soil temperature in the DSR system did not result in an increase of $CH_4$ emissions compared to the TPR system (Fig. 2a, h). After excluding the potential effect of different precipitation, soil temperature and water management practices between the TPR and DSR systems on $F_{CH4}$, the significant increase in $CH_4$ emissions in the DSR compared to the TPR system remained (Fig. 4b). The DSR emitted more methane than the TPR system for the same soil temperature (Fig. 4b). On the contrary, after normalizing $F_{CH4}$ by the ratio of rice aboveground biomass in the DSR and TPR system, no significant difference in $F_{CH4}$ between the DSR and TPR system for the same soil temperature (Fig. 4c). Furthermore, one additional dataset with DSR technology in 2017 was added here for supplementary evidence. The environmental and flux variables in 2017 were very similar to the 2016 conditions except for rainfall. The seasonal total rainfall in 2017 was 484.2 mm, which was higher than 353.5 mm in 2013 and lower than 698.2 mm in 2016. However, the DSR system in 2017 still increased the seasonal $CH_4$

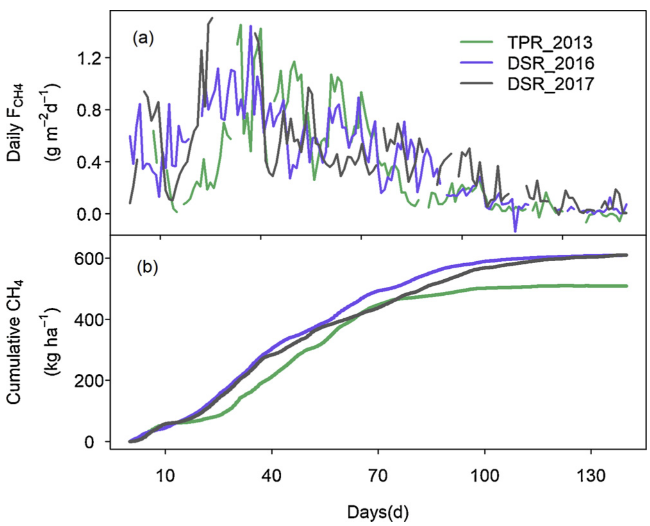


**Fig. 6.** Additional methane flux dataset with DSR technology is added for comparison. Daily $F_{CH4}$ (a) of DSR (*i.e.* DOY 163–315 in 2016 and DOY 158–298 in 2017) and TPR (*i.e.* DOY161 − 309 in 2013) and their cumulative $CH_4$ emissions (b) after transplantation in TPR and after sowing in DSR show that $CH_4$ emissions of both DSR systems are larger than the TPR cropping systems. The TPR system in 2013, the DSR system in 2016 and the DSR system in 2017 are distinguished by green, purple and dark gray colours, respectively (a, b). Cumulative $CH_4$ emissions (b) are derived from gap-filled fluxes (For interpretation of the references to colour in this figure legend, the reader is referred to the web version of this article).

emissions (610.4 kg ha$^{-1}$) by 25% compared to the TPR. These supplementary results indicate that the increase of $CH_4$ emissions in the DSR system compared to the TPR are most likely not due to differences in environmental conditions.

In many ecosystems, $CH_4$ production is fueled by recent plant photosynthate in the form of root exudates in the rhizosphere as shown by $^{14}$C-labeling studies (Dorodnikov et al., 2011; King et al., 2002). Hatala et al (2012a) found that GEP is the primary cause of diurnal patterns in rice paddy $F_{CH4}$. In addition, Knox et al (2016) concluded that GEP and water level typically explain most of the variance in daily average $F_{CH4}$ during the growing season. In our study, we found a significant correlation between $F_{CH4}$ and GEP in both systems before and after the mid-season drainage (Fig. 3). The time lag (Fig. 3a, c) indicates that GEP leads $CH_4$ emissions by 3–7 h in the rice paddy field. Similar to Hatala et al., (2012a,b), we also found that the GEP and $F_{CH4}$ are strongly coherent at the daily scale with a mean time lag of 2.8 h before midseason drainage in the TPR system (Fig. 7). This indicates a simple causality between the GEP and $F_{CH4}$ whose oscillations are phase locked at the daily timescale (Grinsted et al., 2004; Hatala et al., 2012a; Koebsch et al., 2015; Xu et al., 2014). In the DSR system, GEP and $F_{CH4}$ were also coherent at the daily scale, but the significant coherence area was discontinuous (Fig. S3), which may have been caused by large gaps in the $F_{CH4}$ time series from June to July.

Higher GEP is related to increased production of carbon substrates for the methanogenic metabolism and can thus lead to higher $CH_4$ production. GEP differed between the two systems with DSR being more productive (Table 2), resulting in higher $CH_4$ emissions for the same soil temperature in the DSR system. In order to compensate for poor crop establishment and to suppress weed growth, farmers usually adopt a high seeding rate for DSR (Chauhan, 2012; Liu et al., 2014b), which has also been the case for our study site. A higher seeding rate in DSR leads to higher plant density, which can result in higher GEP. The higher plant density can therefore explain why GEP in 2016 was much higher than in 2013. At the same time, increased plant density and aboveground biomass (Table 2) would also result in increased aerenchyma density. Aerenchyma provides a pathway from the root zone to the atmosphere for methane to bypass oxidation layers (Aulakh et al., 2000). Liu et al. (2014a) also found a significant correlation between seasonal total of $CH_4$ emissions and rice biomass. In our study, the change of difference in $F_{CH4}$ for the same soil temperature (5 cm) between the DSR and TPR system before and after the normalization by the ratio of rice aboveground biomass supported this claim. Therefore, the difference in rice plant density was likely the primary reason leading to increased $CH_4$ emissions in the DSR system.

Increasing crop density has been widely proposed as an approach to increase crop competitiveness against weeds, which are the most important constraint to the success of DSR (Chauhan et al., 2017; Liu et al., 2014b). In our case, the wet DSR with prolonged periods of flooding cropping system successfully reduced labor and water consumption, but the increased plant density, aboveground biomass and GEP caused an increase in $CH_4$ emissions compared to the TPR system. Moreover, the rice yield decreased in the DSR system as also reported by previous studies (Farooq et al., 2011, 2007, 2006; Liu et al., 2014b; Naklang et al., 1996). Increasing human population necessitates further increases in rice production to ensure future food security and social stability (Heong and Hardy, 2009). Thus, benefits for rice cropping systems need to be assessed regarding multiple criteria including crop yield and $CH_4$ emission impacts on climate change. Considering the decrease in rice yield and the high radiative forcing of $CH_4$, the benefits of a shift in current rice establishment methods from the conventional TPR to the labor-saving DSR with high-density method need to be carefully re-evaluated in southeast China. However, a better-informed management of planting density and irrigation regime has the potential to limit increases in $CH_4$ emissions of DSR systems.

## 5. Conclusion

For the first time, we analyzed $F_{CH4}$ measured with the eddy covariance technique over two growing seasons (TPR in 2013 vs DSR in 2016) in a rice paddy in southeastern China. The seasonal cumulative $CH_4$ emissions were estimated at 610.5 ± 73.3 kg ha$^{-1}$ and 488.8 ± 56.2 kg ha$^{-1}$ in the DSR and TPR cropping systems, respectively. The hypothesis that direct-seeded rice decrease methane emissions of rice paddies was not supported in our study. Compared to TPR cropping systems, $CH_4$ emissions of the DSR system increased by 25%. After eliminating the effect of differing weather conditions and management practices between the TPR and DSR systems, $CH_4$ emissions in the DSR system during the flooding periods remained much larger than in the TPR system. In contrast, both GEP and rice density were higher in the DSR than in the TPR system. Increased $CH_4$ emissions in the DSR system are most likely due to greater GEP associated with higher rice plant density. Our results highlight the ecological importance of plant density for $CH_4$ emissions in rice paddies. This case study shows that the shift from TPR to wet DSR with higher rice plant density could increase rice seasonal $CH_4$ emissions in paddy fields.

## Acknowledgments

This study was supported by grant from the National Key Research and Development Program of China (Grant No. 2018YFD0900806), the National Natural Science Foundation of China (Grant Nos. 31170450, 30870409, and 40471087), the Key Basic Research Project of the Science and Technology Commission of Shanghai Municipality (13JC1400400), and Research Plan of Shanghai Science and Technology Committee (14ZR1435100). Thanks Zhen-Feng Xu, Jun Ma, Xin-Xin Wang, Shi-Yu Li, De-Rong Xiao, Yong Min for their helpful assistances and advices for the manuscript. Thanks US-China Carbon Consortium (USCCC). Hong Li thanks China Scholarship Council (CSC) for offering a scholarship at the University of Quebec at Montreal (UQAM). We thank the anonymous reviewers for providing insightful comments that improved the quality of the manuscript.

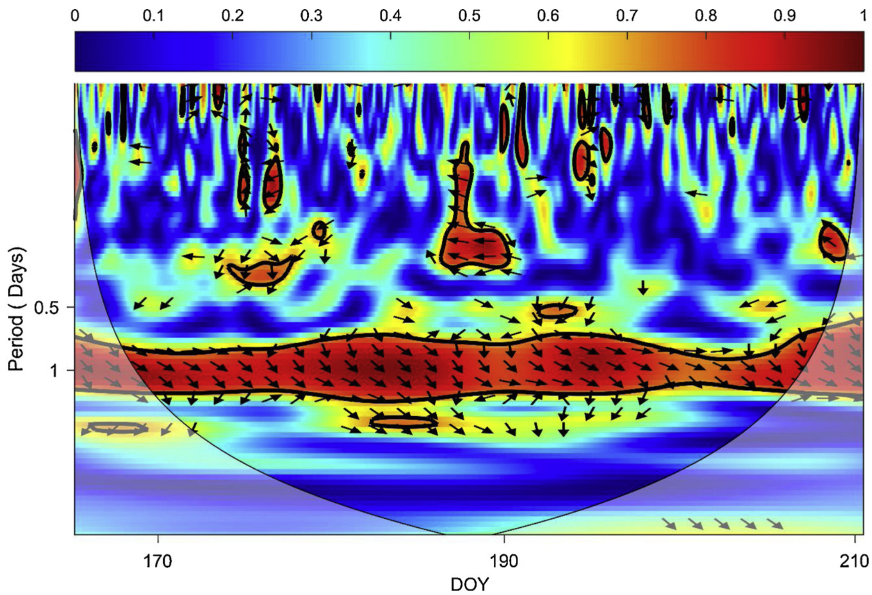


**Fig. 7.** The wavelet coherence between GEP and $F_{CH4}$ for the rice paddy growing season before the practice of mid-season drainage shows high in-phase coherence between the two time series at the daily timescale in the TPR system (2013). The 5% significance level with Monte Carlo simulations of AR-1 autocorrelation is shown as the bold black lines. The cone of influence represents the limit where wavelet power dropped to $e^{-2}$ of the edge values. The direction of arrows presents the phase angle between GEP and $F_{CH4}$ (with in-phase pointing right, anti-phase pointing left. Arrows pointing down are interpreted as $F_{CH4}$ lags GEP).

## Appendix A. Supplementary data

Supplementary material related to this article can be found, in the online version, at doi:https://doi.org/10.1016/j.agrformet.2019.04.005.

## References

Alberto, M.C.R., Wassmann, R., Buresh, R.J., Quilty, J.R., Correa Jr, T.Q., Sandro, J.M., Centeno, C.A.R., 2014. Measuring methane flux from irrigated rice fields by eddy covariance method using open-path gas analyzer. Field Crops Res. 160, 12–21. https://doi.org/10.1016/j.fcr.2014.02.008.

Alberto, M.C.R., Wassmann, R., Gummert, M., Buresh, R.J., Quilty, J.R., Correa Jr, T.Q., Centeno, C.A.R., Oca, G.M., 2015. Straw incorporated after mechanized harvesting of irrigated rice affects net emissions of $CH_4$ and $CO_2$ based on eddy covariance measurements. Field Crops Res. 184, 162–175. https://doi.org/10.1016/j.fcr.2015.10.004.

Aulakh, M.S., Wassmann, R., Rennenberg, H., Fink, S., 2000. Pattern and amount of aerenchyma relate to variable methane transport capacity of different rice cultivars. Plant Biol. 2, 182–194. https://doi.org/10.1055/s-2000-9161.

Aurela, M., Laurila, T., Tuovinen, J., 2002. Annual $CO_2$ balance of a subarctic fen in northern Europe: importance of the wintertime efflux. J. Geophys. Res. Atmos. 107.

Baldocchi, D., Falge, E., Wilson, K., 2001. A spectral analysis of biosphere–atmosphere trace gas flux densities and meteorological variables across hour to multi-year time scales. Agric. For. Meteorol. 107, 1–27. https://doi.org/10.1016/S0168-1923(00)00228-8.

Bhattacharyya, P., Neogi, S., Roy, K.S., Dash, P.K., Nayak, A.K., Mohapatra, T., 2014. Tropical low land rice ecosystem is a net carbon sink. Agric. Ecosyst. Environ. 189, 127–135. https://doi.org/10.1016/j.agee.2014.03.013.

Bracewell, Newbold, Ronald, Bracewell, Ronald, N., 1986. The Fourier Transform and Its Applications. McGraw-Hill, New York.

Chauhan, B.S., 2012. Weed management in direct-seeded rice systems. Int. Rice Res. Inst.

Chauhan, B.S., Jabran, K., Mahajan, G. (Eds.), 2017. Rice Production Worldwide. Springer International Publishing, Cham.. https://doi.org/10.1007/978-3-319-47516-5.

Chen, F., Chen, P., 2011. Present status and evaluation of economic benefits of direct-seeded rice in south China. Chin. Rice 1–5.

Conrad, R., 2007. Microbial Ecology of Methanogens and Methanotrophs, in: Advances in Agronomy, Advances in Agronomy. Academic Press, pp. 1–63. https://doi.org/10.1016/S0065-2113(07)96005-8.

Conrad, R., 1996. Soil microorganisms as controllers of atmospheric trace gases ($H_2$, CO, $CH_4$, OCS, $N_2O$, and NO). Microbiol. Rev. 60, 609–640.

Cui, J., Liu, C., Li, Z., Wang, L., Chen, X., Ye, Z., Fang, C., 2012. Long-term changes in topsoil chemical properties under centuries of cultivation after reclamation of coastal wetlands in the Yangtze Estuary. China. Soil Tillage Res. 123, 50–60. https://doi.org/10.1016/j.still.2012.03.009.

Detto, M., Verfaillie, J., Anderson, F., Xu, L., Baldocchi, D., 2011. Comparing laser-based open- and closed-path gas analyzers to measure methane fluxes using the eddy covariance method. Agric. For. Meteorol. 151, 1312–1324. https://doi.org/10.1016/j.agrformet.2011.05.014.

Dore, S., Hymus, G.J., Johnson, D.P., Hinkle, C.R., Valentini, R., Drake, B.G., 2003. Cross validation of open-top chamber and eddy covariance measurements of ecosystem $CO_2$ exchange in a Florida scrub-oak ecosystem. Glob. Change Biol. Bioenergy 9, 84–95. https://doi.org/10.1046/j.1365-2486.2003.00561.x.

Farooq, M., Basra, S.M.A., Tabassum, R., Afzal, I., 2006. Enhancing the performance of direct seeded fine rice by seed priming. Plant Prod. Sci. 9, 446–456. https://doi.org/10.1626/pps.9.446.

Farooq, M., Basra, S.M.A., Ahmad, N., 2007. Improving the performance of transplanted rice by seed priming. Plant Growth Regul. 51, 129–137. https://doi.org/10.1007/s10725-006-9155-x.

Farooq, M., Siddique, K.H.M., Rehman, H., Aziz, T., Lee, D.-J., Wahid, A., 2011. Rice direct seeding: experiences, challenges and opportunities. Soil Tillage Res. 111, 87–98. https://doi.org/10.1016/j.still.2010.10.008.

Finkelstein, P.L., Sims, P.F., 2001. Sampling error in eddy correlation flux measurements. J. Geophys. Res.-Atmospheres 106, 3503–3509. https://doi.org/10.1029/2000jd900731.

Foken, T., Gockede, M., Mauder, M., Mahrt, L., Amiro, B., Munger, W., 2004. Post-field data quality control. Handbook of Micrometeorology: A Guide for Surface Flux Measurement and Aanlysis. pp. 181–208.

Ge, H.-X., Zhang, H.-S., Zhang, H., Cai, X.-H., Song, Y., Kang, L., 2018. The characteristics of methane flux from an irrigated rice farm in East China measured using the eddy covariance method. Agric. For. Meteorol. 249, 228–238. https://doi.org/10.1016/j.agrformet.2017.11.010.

Grinsted, A., Moore, J.C., Jevrejeva, S., 2004. Application of the cross wavelet transform and wavelet coherence to geophysical time series. Nonlinear Process. Geophys. 11, 561–566.

Gu, S., Li, G., Zhang, Q., Shen, X., Yuan, W., Zuo, J., Cheng, T., Shen, J., 2015. Tillering characteristics and relations between tillering and yield components of machine-sown rice following wheat in Shanghai. Acta Agric. Shanghai 117–121.

Gupta, D.K., Bhatia, A., Kumar, A., Das, T.K., Jain, N., Tomer, R., Malyan, S.K., Fagodiya, R.K., Dubey, R., Pathak, H., 2016. Mitigation of greenhouse gas emission from rice–wheat system of the Indo-Gangetic plains: through tillage, irrigation and fertilizer management. Agric. Ecosyst. Environ. 230, 1–9. https://doi.org/10.1016/j.agee.2016.05.023.

Hang, X., Zhang, X., Song, C., Jiang, Y., Deng, A., He, R., Lu, M., Zhang, W., 2014. Differences in rice yield and $CH_4$ and $N_2O$ emissions among mechanical planting methods with straw incorporation in Jianghuai area, China. Soil Tillage Res. 144, 205–210. https://doi.org/10.1016/j.still.2014.07.013.

Hatala, J.A., Detto, M., Baldocchi, D.D., 2012a. Gross ecosystem photosynthesis causes a diurnal pattern in methane emission from rice. Geophys. Res. Lett. 39, L06409. https://doi.org/10.1029/2012GL051303.

Hatala, J.A., Detto, M., Sonnentag, O., Deverel, S.J., Verfaillie, J., Baldocchi, D.D., 2012b. Greenhouse gas ($CO_2$, $CH_4$, $H_2O$) fluxes from drained and flooded agricultural peatlands in the Sacramento-San Joaquin Delta. Agric. Ecosyst. Environ. 150, 1–18. https://doi.org/10.1016/j.agee.2012.01.009.

Helbig, M., Chasmer, L.E., Kljun, N., Quinton, W.L., Treat, C.C., Sonnentag, O., 2017. The positive net radiative greenhouse gas forcing of increasing methane emissions from a thawing boreal forest-wetland landscape. Glob. Change Biol. Bioenergy 23, 2413–2427. https://doi.org/10.1111/gcb.13520.

Heong, K.L., Hardy, B., 2009. Planthoppers: new threats to the sustainability of intensive rice production systems in Asia. Int. Rice Res. Inst.

Hommeltenberg, J., Mauder, M., Droesler, M., Heidbach, K., Werle, P., Schmid, H.P., 2014. Ecosystem scale methane fluxes in a natural temperate bog-pine forest in southern Germany. Agric. For. Meteorol. 198, 273–284. https://doi.org/10.1016/j.agrformet.2014.08.017.

Hou, H., Peng, S., Xu, J., Yang, S., Mao, Z., 2012. Seasonal variations of $CH_4$ and $N_2O$ emissions in response to water management of paddy fields located in Southeast China. Chemosphere 89, 884–892. https://doi.org/10.1016/j.chemosphere.2012.04.066.

Kim, Y., Talucder, M.S.A., Kang, M., Shim, K.-M., Kang, N., Kim, J., 2016. Interannual variations in methane emission from an irrigated rice paddy caused by rainfalls during the aeration period. Agric. Ecosyst. Environ. 223, 67–75. https://doi.org/10.1016/j.agee.2016.02.032.

Knox, S.H., Sturtevant, C., Matthes, J.H., Koteen, L., Verfaillie, J., Baldocchi, D., 2015. Agricultural peatland restoration: effects of land-use change on greenhouse gas ($CO_2$ and $CH_4$) fluxes in the Sacramento-San Joaquin Delta. Glob. Change Biol. Bioenergy 21, 750–765. https://doi.org/10.1111/gcb.12745.

Knox, S.H., Matthes, J.H., Sturtevant, C., Oikawa, P.Y., Verfaillie, J., Baldocchi, D., 2016. Biophysical controls on interannual variability in ecosystem-scale $CO_2$ and $CH_4$ exchange in a California rice paddy. J. Geophys. Res. Biogeosciences 121https://doi.org/10.1002/2015JG003247. 2015JG003247.

Koebsch, F., Jurasinski, G., Koch, M., Hofmann, J., Glatzel, S., 2015. Controls for multi-scale temporal variation in ecosystem methane exchange during the growing season of a permanently inundated fen. Agric. For. Meteorol. 204, 94–105. https://doi.org/10.1016/j.agrformet.2015.02.002.

Krauss, K.W., Holm, G.O., Perez, B.C., McWhorter, D.E., Cormier, N., Moss, R.F., Johnson, D.J., Neubauer, S.C., Raynie, R.C., 2016. Component greenhouse gas fluxes and radiative balance from two deltaic marshes in Louisiana: Pairing chamber techniques and eddy covariance. J. Geophys. Res. Biogeosciences 121, 1503–1521.

Kumar, V., Ladha, J.K., 2011. Direct seeding of rice: recent developments and future research needs. Adv. Agron. 111, 13.

Lasslop, G., Reichstein, M., Papale, D., Richardson, A.D., Arneth, A., Barr, A., Stoy, P., Wohlfahrt, G., 2010. Separation of net ecosystem exchange into assimilation and respiration using a light response curve approach: critical issues and global evaluation. Glob. Change Biol. Bioenergy 16, 187–208. https://doi.org/10.1111/j.1365-2486.2009.02041.x.

Li, C., Qiu, J., Frolking, S., Xiao, X., Salas, W., Moore, B., Boles, S., Huang, Y., Sass, R., 2002. Reduced methane emissions from large-scale changes in water management of China's rice paddies during 1980–2000. Geophys. Res. Lett. 29, 1972. https://doi.org/10.1029/2002GL015370.

Li, H., Dai, S., Ouyang, Z., Xie, X., Guo, H., Gu, C., Xiao, X., Ge, Z., Peng, C., Zhao, B., 2018. Multi-scale temporal variation of methane flux and its controls in a subtropical tidal salt marsh in eastern China. Biogeochemistry 137, 163–179. https://doi.org/10.1007/s10533-017-0413-y.

Liu, Q., 2016. Study on the Weed Seedbank in Direct-seeding Rice Field and Integrated Management of Chinese Sprangletop (Leptochloa Chinensis) in the Lower-middle Reaches of the Yangze River.

Liu, S., Zhang, Y., Lin, F., Zhang, L., Zou, J., 2014a. Methane and nitrous oxide emissions from direct-seeded and seedling-transplanted rice paddies in southeast China. Plant Soil 374, 285–297. https://doi.org/10.1007/s11104-013-1878-7.

Liu, H., Hussain, S., Zheng, M., Sun, L., Fahad, S., Huang, J., Cui, K., Nie, L., 2014b. Progress and constraints of dry direct-seeded rice in China. J. Food Agric. Environ. 12, 465–472.

Liu, H., Hussain, S., Zheng, M., Peng, S., Huang, J., Cui, K., Nie, L., 2015. Dry direct-seeded rice as an alternative to transplanted-flooded rice in Central China. Agron. Sustain. Dev. 35, 285–294. https://doi.org/10.1007/s13593-014-0239-0.

Malyan, S.K., Bhatia, A., Kumar, A., Gupta, D.K., Singh, R., Kumar, S.S., Tomer, R., Kumar, O., Jain, N., 2016. Methane production, oxidation and mitigation: a mechanistic understanding and comprehensive evaluation of influencing factors. Sci. Total Environ. 572, 874–896. https://doi.org/10.1016/j.scitotenv.2016.07.182.

Meijide, A., Manca, G., Goded, I., Magliulo, V., di Tommasi, P., Seufert, G., Cescatti, A., 2011. Seasonal trends and environmental controls of methane emissions in a rice paddy field in Northern Italy. Biogeosciences 8, 3809–3821. https://doi.org/10.5194/bg-8-3809-2011.

Meijide, A., Gruening, C., Goded, I., Seufert, G., Cescatti, A., 2017. Water management reduces greenhouse gas emissions in a Mediterranean rice paddy field. Agric. Ecosyst. Environ. 238, 168–178. https://doi.org/10.1016/j.agee.2016.08.017. Quantification and mitigation of greenhouse gas emissions in Mediterranean cropping systems.

Moncrieff, J., Valentini, R., Greco, S., Guenther, S., Ciccioli, P., 1997. Trace gas exchange over terrestrial ecosystems: methods and perspectives in micrometeorology. J. Exp. Bot. 48, 1133–1142.

Morin, T.H., Bohrer, G., Stefanik, K.C., Rey-Sanchez, A.C., Matheny, A.M., Mitsch, W.J., 2017. Combining eddy-covariance and chamber measurements to determine the methane budget from a small, heterogeneous urban floodplain wetland park. Agric. For. Meteorol. 237–238, 160–170. https://doi.org/10.1016/j.agrformet.2017.01.022.

Naklang, K., Shu, F., Nathabut, K., 1996. Growth of rice cultivars by direct seeding and transplanting under upland and lowland conditions. Field Crops Res. 48, 115–123. https://doi.org/10.1016/S0378-4290(96)01029-5.

Nie, L., Peng, S., 2017. Rice Production in China. Rice Production Worldwide. Springer, Cham, pp. 33–52. https://doi.org/10.1007/978-3-319-47516-5_2.

Papoulis, A., Maradudin, A.A., 1963. The fourier integral and its applications. Phys. Today 16, 70.

Pathak, H., 2012. Greenhouse Gas Emission From Agriculture. Carbon Manag. Agric. Mitigating Greenh. Eff. Springer, UK, pp. 60–69.

Pathak, H., Tewari, A.N., Sankhyan, S., Dubey, D.S., Mina, U., Singh, V.K., Jain, N., Bhatia, A., 2011. Direct-seeded rice: potential, performance and problems–a review. Curr. Adv. Agric. Sci. 3, 77–88.

Rao, A.N., Johnson, D.E., Sivaprasad, B., Ladha, J.K., Mortimer, A.M., 2007. Weed management in direct-seeded rice. In: Sparks, D.L. (Ed.), Advances in Agronomy. Academic Press, pp. 153–255. https://doi.org/10.1016/S0065-2113(06)93004-1.

Reichstein, M., Falge, E., Baldocchi, D., Papale, D., Aubinet, M., Berbigier, P., Bernhofer, C., Buchmann, N., Gilmanov, T., Granier, A., Grünwald, T., Havránková, K., Ilvesniemi, H., Janous, D., Knohl, A., Laurila, T., Lohila, A., Loustau, D., Matteucci, G., Meyers, T., Miglietta, F., Ourcival, J.-M., Pumpanen, J., Rambal, S., Rotenberg, E., Sanz, M., Tenhunen, J., Seufert, G., Vaccari, F., Vesala, T., Yakir, D., Valentini, R., 2005. On the separation of net ecosystem exchange into assimilation and ecosystem respiration: review and improved algorithm. Glob. Change Biol. Bioenergy 11, 1424–1439. https://doi.org/10.1111/j.1365-2486.2005.001002.x.

Sandhu, N., Kumar, A., 2016. Paper 16 Traits for dry direct-seeded rice. Reg. Dev. Dissem. Clim.-Resilient Rice Var. Water-Short Areas South Asia Southeast Asia 378.

Smith, P., Martino, D., Cai, Z., I.P. on C.C.W, et al., 2007. Climate Change 2007: Mitigation: Contribution of Working Group III to the Fourth Assessment Report of the Intergovernmental Panel on Climate Change: Summary for Policymakers and Technical Summary. Cambridge University Press.

Sudhir-Yadav, Humphreys, E., Kukal, S.S., Gill, G., Rangarajan, R., 2011. Effect of water management on dry seeded and puddled transplanted rice: part 2: water balance and water productivity. Field Crops Res. 120, 123–132. https://doi.org/10.1016/j.fcr.2010.09.003.

Tao, Y., Chen, Q., Peng, S., Wang, W., Nie, L., 2016. Lower global warming potential and higher yield of wet direct-seeded rice in Central China. Agron. Sustain. Dev. 36, 24. https://doi.org/10.1007/s13593-016-0361-2.

Torrence, C., Compo, G.P., 1998. A practical guide to wavelet analysis. Bull. Am. Meteorol. Soc. 79, 61–78. https://doi.org/10.1175/1520-0477(1998)079<0061:APGTWA>2.0.CO;2.

Vickers, D., Mahrt, L., 1997. Quality control and flux sampling problems for tower and aircraft data. J. Atmospheric Ocean. Technol. 14, 512–526.

Wang, X., Gan, J., Zhu, M., Zhao, Z., Li, M., Zhou, D., Cao, L., 2017. Research and application of the rice precision hill-drop drilling technology in Shanghai. China Rice 168–172.

Webb, E.K., Pearman, G.I., Leuning, R., 1980. Correction of flux measurements for density effects due to heat and water vapour transfer. Q. J. R. Meteorol. Soc. 106, 85–100.

Wilczak, J.M., Oncley, S.P., Stage, S.A., 2001. Sonic anemometer tilt correction algorithms. Bound.-Layer Meteorol. 99, 127–150. https://doi.org/10.1023/A:1018966204465.

Xu, L., Lin, X., Amen, J., Welding, K., McDermitt, D., 2014. Impact of changes in barometric pressure on landfill methane emission. Glob. Biogeochem. Cycles 28https://doi.org/10.1002/2013GB004571. 2013GB004571.

Yu, L.F., Wang, H., Wang, G.S., Song, W.M., Huang, Y., Li, S.G., Liang, N.S., Tang, Y.H., He, J.S., 2013. A comparison of methane emission measurements using eddy covariance and manual and automated chamber-based techniques in Tibetan Plateau alpine wetland. Environ. Pollut. 181, 81–90. https://doi.org/10.1016/j.envpol.2013.06.018.

Yvon-Durocher, G., Allen, A.P., Bastviken, D., Conrad, R., Gudasz, C., St-Pierre, A., Thanh-Duc, N., del Giorgio, P.A., 2014. Methane fluxes show consistent temperature dependence across microbial to ecosystem scales. Nature 507, 488–491. https://doi.org/10.1038/nature13164.

Zhang, A., Bian, R., Pan, G., Cui, L., Hussain, Q., Li, L., Zheng, Jinwei, Zheng, Jufeng, Zhang, X., Han, X., Yu, X., 2012. Effects of biochar amendment on soil quality, crop yield and greenhouse gas emission in a Chinese rice paddy: a field study of 2 consecutive rice growing cycles. Field Crops Res. 127, 153–160. https://doi.org/10.1016/j.fcr.2011.11.020.

Zou, J., Huang, Y., Jiang, J., Zheng, X., Sass, R.L., 2005. A 3-year field measurement of methane and nitrous oxide emissions from rice paddies in China: effects of water regime, crop residue, and fertilizer application. Glob. Biogeochem. Cycles 19, GB2021. https://doi.org/10.1029/2004GB002401.